ONLINE APPENDIX

Supplemental Fig. S1. An acute ablation of *Perk* function leads to an ER to Golgi anterograde trafficking defect. Immunohistochemistry in HepG2 cells (**A-C**), AD293 cells (**D-E**). *ts045* VSVG-GFP was co-transfected with an empty vector into HepG2 cells. Cells were incubated overnight at the restrictive temperature (40°C) to allow the cargo to accumulate in the ER. Cells were then shifted to the permissive temperature (32°C) for 15 minutes to allow the protein to traffic to the Golgi. Dashed line indicates *ts045* VSVG-GFP (green, **A**) transfected cell. Staining for the Golgi marker GM130 is shown in red (**B**) and the merged image is seen in **C**. Similarly, successful trafficking of the VSVG cargo (green) to the Golgi is seen in empty vector co-transfected AD293 cells (**D**). However, an ablation of *Perk* function in *ts045* VSVG-GFP (green) and cmyc-tagged *DNPerk* (red) co-transfected AD293 cells shows a large number of impacted-ER-like cells (**E**).

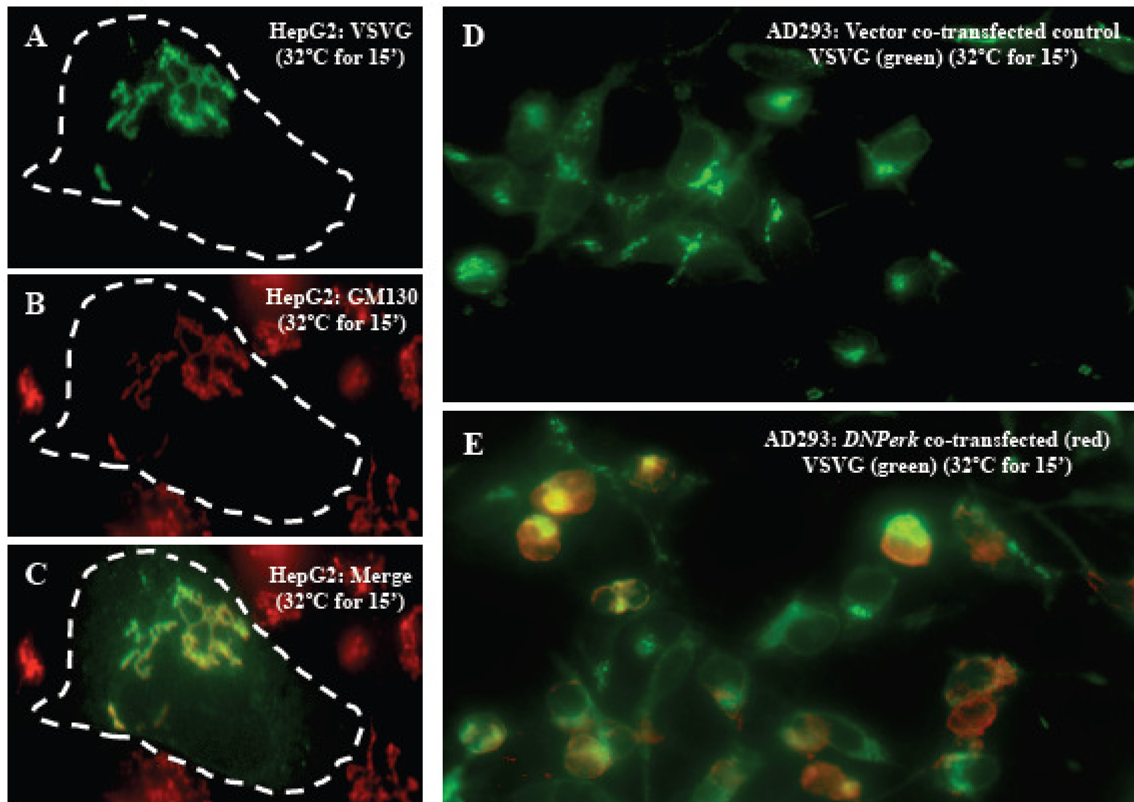

©2010 American Diabetes Association. Published online at http://diabetes.diabetesjournals.org/cgi/content/full/db09-1064/DC1.

Supplemental Fig. S2. HA tagged S2P redistributes to the ER (A-D). Immunohistochemistry in AD293 cells (**A**-**D**). Cells were cultured and prepared for IHC as described in Fig 2. **A:** Normal Golgi localization of HA tagged S2P (red). Nuclear staining with DAPI is shown in blue. **B-D:** c-myc-tagged *DNPerk* is shown in green (**B**) and the merged image with HA-S2P (red, **C**) is shown in **D**. Arrows show normal Golgi localization of HA-S2P and the arrowheads indicate the ER redistribution of HA-S2P in *DNPerk* co-transfected cells. The results of these experiments need to be confirmed by ablating *Perk* mRNA expression by use of siRNA knockdown.

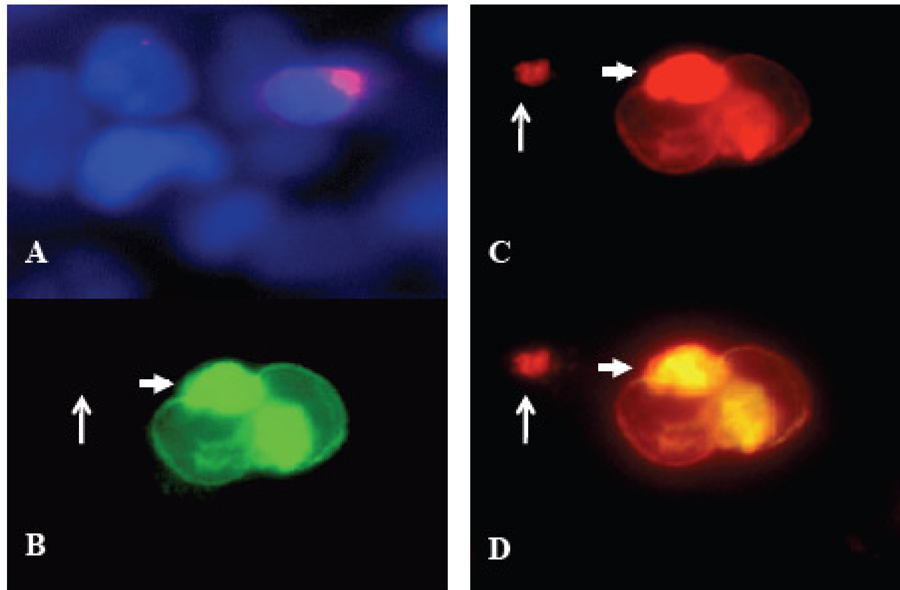

©2010 American Diabetes Association. Published online at http://diabetes.diabetesjournals.org/cgi/content/full/db09-1064/DC1.

Supplemental Fig. S3. Loss of PERK function leads to alterations in ER and Golgi sterol composition. Representative data from two independent experiments involving subcellular fractionation in *Perk*-ablated AD293 cells is shown. SCF was carried out as described in Fig. 3. Fractions were extracted with an equal volume of chloroform:methanol (9:1) followed by evaporation of the organic phase. The residue was resuspended in the appropriate buffer for the cholesterol assay, which was carried out using the Biovision Cholesterol Quantitation Kit. **A-B:** Cholesterol content of membrane fractions in *Perk*-ablated cells (solid line) and non-ablated vector controls (dashed line). The ER fractions (enriched in fractions 6-10) and the Golgi (enriched in fractions 2-5) were analyzed for total (**A**) and esterified cholesterol (**B**) following the instructions provided in the kit. Acute ablation of *Perk* resulted in a large increase in the total cholesterol content in the ER of *Perk*-ablated AD293 cells and a corresponding decrease in the Golgi amplifying the disparity in cholesterol content between them (**A**). Further analysis revealed that esterified cholesterol accounted for 74.3% of the total Golgi cholesterol (fraction 4) and 2.6% of the ER cholesterol (fraction 9) in the control cells (**B**). In contrast, esterified cholesterol accounted for 21.2% of the total ER cholesterol content (fraction 9) in *Perk*-deficient cells (**B**).

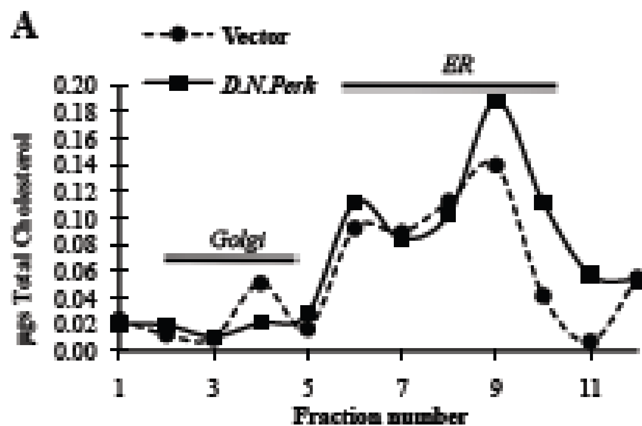

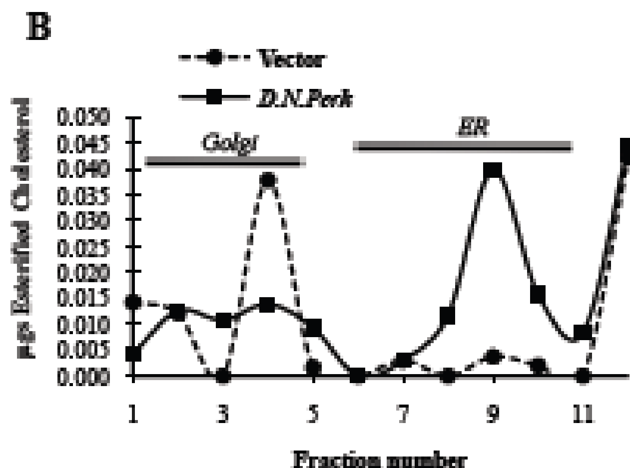

©2010 American Diabetes Association. Published online at http://diabetes.diabetesjournals.org/cgi/content/full/db09-1064/DC1.

Supplemental Fig. S4. Impaired ERAD in *Perk*-deficient cells. Immunohistochemistry in AD293 cells (**A-B**). Cells were transfected with either V5 epitope tagged wild-type proinsulin that showed a punctate, perinuclear Golgi localization (arrow, red, **A**) or V5 epitope tagged wild-type proinsulin-KDEL that showed ER-localization (arrowhead, red, **B**). Staining for the ER marker Calnexin is shown in green (**A**, **B**). **C:** Proinsulin synthesis rates in AD293 cells cultured in 11.1mM glucose. These cells were cotransfected with *Ins*$^+$-KDEL with either empty vector or *DNPerk*. Cells were then pulsed with S^{35} labeled cysteine and methionine for 30 minutes followed by an immunoprecipitation of the V5-tagged proinsulin. Quantification of autoradiogram signals is shown at the bottom of the panel and represents proinsulin synthesis independent of secretion. **D:** Increased ER-retention of V5-tagged *Ins*$^+$-KDEL in *Perk*-ablated AD293 cells. *Ins*$^+$-KDEL was co-transfected with either empty vector or *DNPerk* and separated into cytosolic (C) and ER (ER) fractions and immunoblotted for calnexin (ER marker), tubulin (cytosolic marker) and the V5 tag. Increased ER-retention of ubiquitylated species is seen in *Perk*-ablated cells. **E:** AD293 cells were transfected with V5 tagged wild-type (Ins$^+$) or mutant (Ins^M) proinsulin (the latter bearing a *C(B19)A* point mutation that effectively leaves the A20 cysteine unpaired (Liu et al. 2005 J. Biol. Chem 280:13209.) following transfection with empty vector (Vector) or *DNPerk*. Lysates were immunoblotted with the anti-V5 antibody. Arrowhead indicates V5-tagged proinsulin. Multiple higher MW bands (arrow) are ubiquitylated proinsulin species as seen in **Fig. 5D**. Quantification of ubiquitylated bands indicates a 62% increase in ubiquitylated proinsulin (normalized to total proinsulin) in *Perk*-ablated cells over empty vector controls.

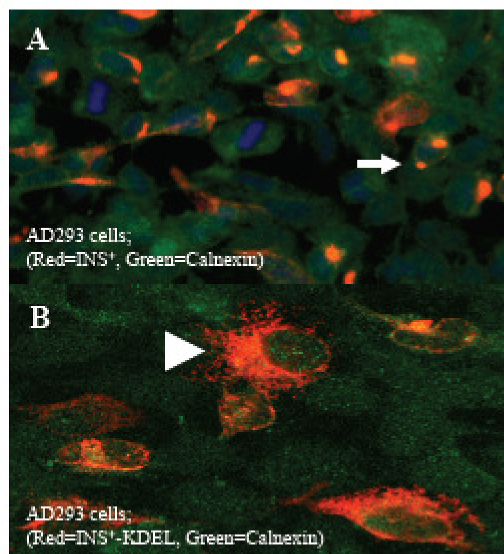

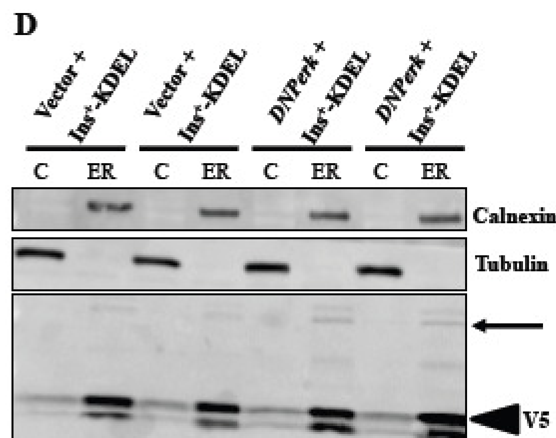

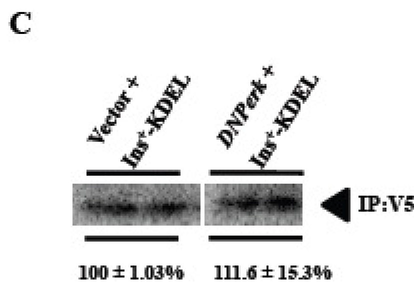

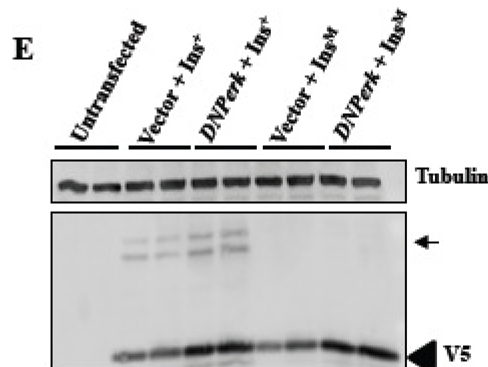

©2010 American Diabetes Association. Published online at http://diabetes.diabetesjournals.org/cgi/content/full/db09-1064/DC1.

Supplemental Fig S5. Proinsulin and insulin content is reduced in the islets of *Akita* mutants and increasing the *Perk* gene dosage accelerates the progression to diabetes in the *Ins2*$^{+/Akita}$ mutants. A&D: Islet immunohistochemistry for 21-day-old *Ins*$^{+/+}$ **B&E**: *Ins2*$^{+/Akita}$ & **C&F:** *Ins2*$^{Akita/Akita}$ littermates. Red=proinsulin; Blue=glucagon; Green=insulin. The signal intensity for glucagon (blue) has been kept uniform for all the panels and the relative proinsulin (red, A-C) and insulin (green, D-F) signal is shown.

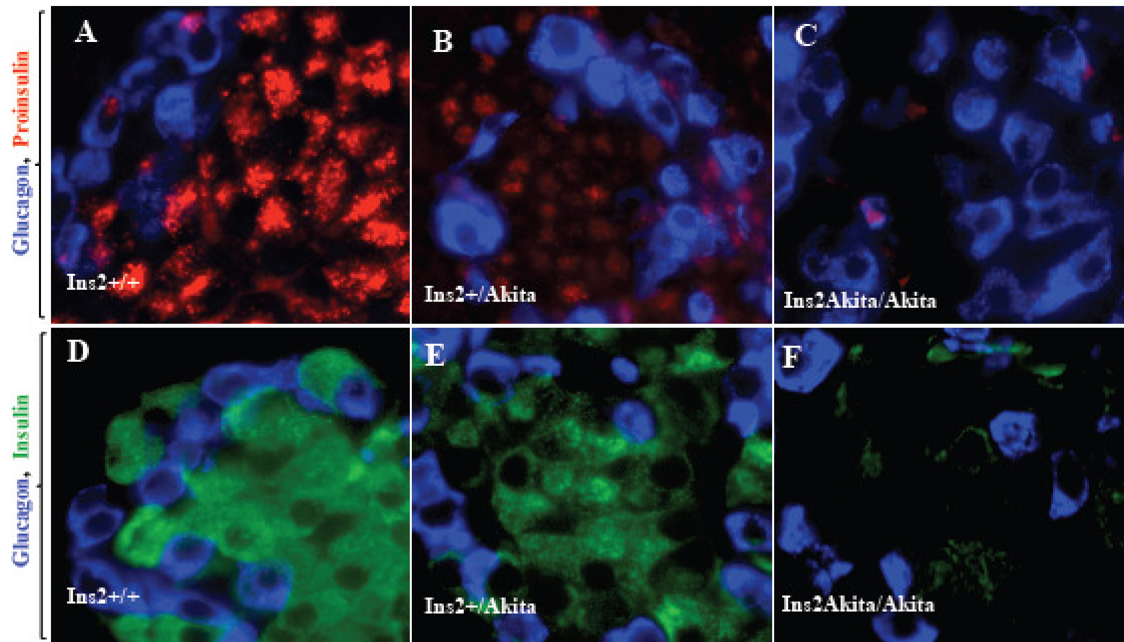

©2010 American Diabetes Association. Published online at http://diabetes.diabetesjournals.org/cgi/content/full/db09-1064/DC1.